Continuous monitoring of dsDNA fragments for biomanufacturing

Biosensors and Bioelectronics 288 (2025) 117808

Contents lists available at ScienceDirect

Biosensors and Bioelectronics

journal homepage: www.elsevier.com/locate/bios

Continuous monitoring of dsDNA fragments for biomanufacturing: Sensor development and feasibility study

Selina A.J. Janssen [a,c], Arthur M. de Jong [b,c], Menno W.J. Prins [a,b,c,d,*]

[a] Department of Biomedical Engineering, Eindhoven University of Technology, 5612 AZ, Eindhoven, the Netherlands
[b] Department of Applied Physics and Science Education, Eindhoven University of Technology, 5612 AZ, Eindhoven, the Netherlands
[c] Institute for Complex Molecular Systems (ICMS), Eindhoven University of Technology, 5612 AZ, Eindhoven, the Netherlands
[d] Helia Biomonitoring B.V., 5612 AR, Eindhoven, the Netherlands

A B S T R A C T

Biomanufacturing processes based on cellular systems are difficult to set up and control due to variabilities in the bioreactor (upstream processing) and in the extraction and purification steps thereafter (downstream processing). For better understanding, monitoring, and control of these processes, sensors are needed that can measure biomolecular constituents such as small molecules, proteins, and nucleic acids. Here, we describe the development of a continuous sensor to monitor host cell DNA, which can function as a marker for cell death in upstream processing and as a marker for product impurity in downstream processing. We present a sensor for the measurement of double-stranded DNA fragments (dsDNA) using anti-dsDNA antibodies in a continuous biosensor based on particle motion with a competition format. Experimental results show that the sensor has reversible interactions with dsDNA fragments of different base pair lengths and gives responses in nano- and micromolar concentration ranges. Particles with varying motion behaviors are distinguished, and their dose-response characteristics are compared. Finally, fluctuating dsDNA concentrations are measured, and the next steps are defined for the development of sensors for the continuous monitoring of host cell DNA in biomanufacturing processes.

1. Introduction

Biomanufacturing processes use living cells and their components to produce, for example, biopharmaceuticals, viral vectors, and cell-based therapeutics (Zhang et al., 2017). These bioprocesses are complex and, therefore, require in-depth investigations to identify origins of variabilities and ensure consistent product quality (Rathore, 2016), (Wasalathanthri et al., 2020), (Isoko et al., 2024), (Sathiyapriyan et al., 2025). Analytical technologies are essential to quantify the underlying process parameters to assure product quality, prevent batch rejections, improve materials use, and optimize production time. Optimized process control is achieved when measurement data are generated automatically using continuous sensors, eliminating delays associated with off-site laboratory analysis (Alford, 2006), (Reyes et al., 2022), (Veloso and Ferreira, 2017). Continuous sensors are commercially available for measuring physical parameters, such as temperature and pressure, and for a few chemical parameters, such as glucose concentration, dissolved oxygen, and pH (Becker et al., 2006), (Glindkamp et al., 2009). However, for monitoring small organic molecules, proteins, and nucleic acids in biomanufacturing processes, continuous sensors are not yet available on the market. It is challenging to develop continuous sensors for such biomolecules as they are present at low concentrations, typically at micromolar concentrations and below.

Continuous sensors that could monitor the status of cells in a bioreactor would offer opportunities for advanced process control. An important phenomenon to monitor is cell death, as this can relate to physiological processes in the cells as well as to detrimental conditions in the bioreactor (Grilo and Mantalaris, 2019), (Wu et al., 2023). Cell death can be detected by measuring the release of membrane and intracellular components into the bioreactor, including host cell proteins (HCP) and host cell DNA (HCD). These molecules are relevant to measure inside the bioreactor (upstream processing) as well as in extraction and purification steps thereafter (downstream processing) for improving both process control and product safety (Grilo and Mantalaris, 2019), (U.S. Food and Drug Administration (FDA) and & Center for Biologics Evaluation and Research (CBER), 2010), (World Health Organization (WHO) and & WHO Expert Committee on Biological Standardization, 2014).

HCD can be quantified as the total mass of extracellular DNA fragments in a sample (Wang et al., 2012). Upon cell death, the genomic DNA of the cells is fragmented by the cell death process itself as well as by shear forces in the bioreactor (Matassov et al., 2004), (Rolinger et al.,

This article is part of a special issue entitled: Continuous Monitoring Biosensors published in Biosensors and Bioelectronics.

* Corresponding author. Department of Biomedical Engineering, Eindhoven University of Technology, 5612 AZ, Eindhoven, the Netherlands.
E-mail address: m.w.j.prins@tue.nl (M.W.J. Prins).

https://doi.org/10.1016/j.bios.2025.117808
Received 13 February 2025; Received in revised form 30 June 2025; Accepted 19 July 2025
Available online 21 July 2025

2020). The golden standard for HCD quantification is quantitative PCR (qPCR) due to its high measurement sensitivity (Wang et al., 2012), (Nissom, 2007), (Zheng et al., 2019). However, PCR uses sequence-specific primers, restricting its ability to quantify total genomic DNA irrespective of sequence. Moreover, qPCR requires extensive sample preparation and consumes biochemical reagents during amplification, complicating the use of qPCR for continuous monitoring applications. DNA intercalating dye assays quantify DNA by sequence-independent binding (Ikeda et al., 2009), (Lauro et al., 2023). However, these methodologies also consume reagents for every sample measured, which is not ideal for continuous monitoring applications.

Here, we report on the development of a strategy for continuously monitoring dsDNA fragments based on Biosensing by Particle Motion (BPM), a continuous biosensing technology with single-molecule resolution (Buskermolen et al., 2022), (Visser et al., 2018). BPM is based on biofunctionalized particles that interact with a biofunctionalized sensing surface, with continuous measurement of the diffusive Brownian motion properties of the particles. Earlier we developed two sensor variants: t-BPM (Visser et al., 2018) (with a tether molecule between particle and surface) and f-BPM (Buskermolen et al., 2022) (without a tether molecule between particle and surface). For the present proof-of-concept

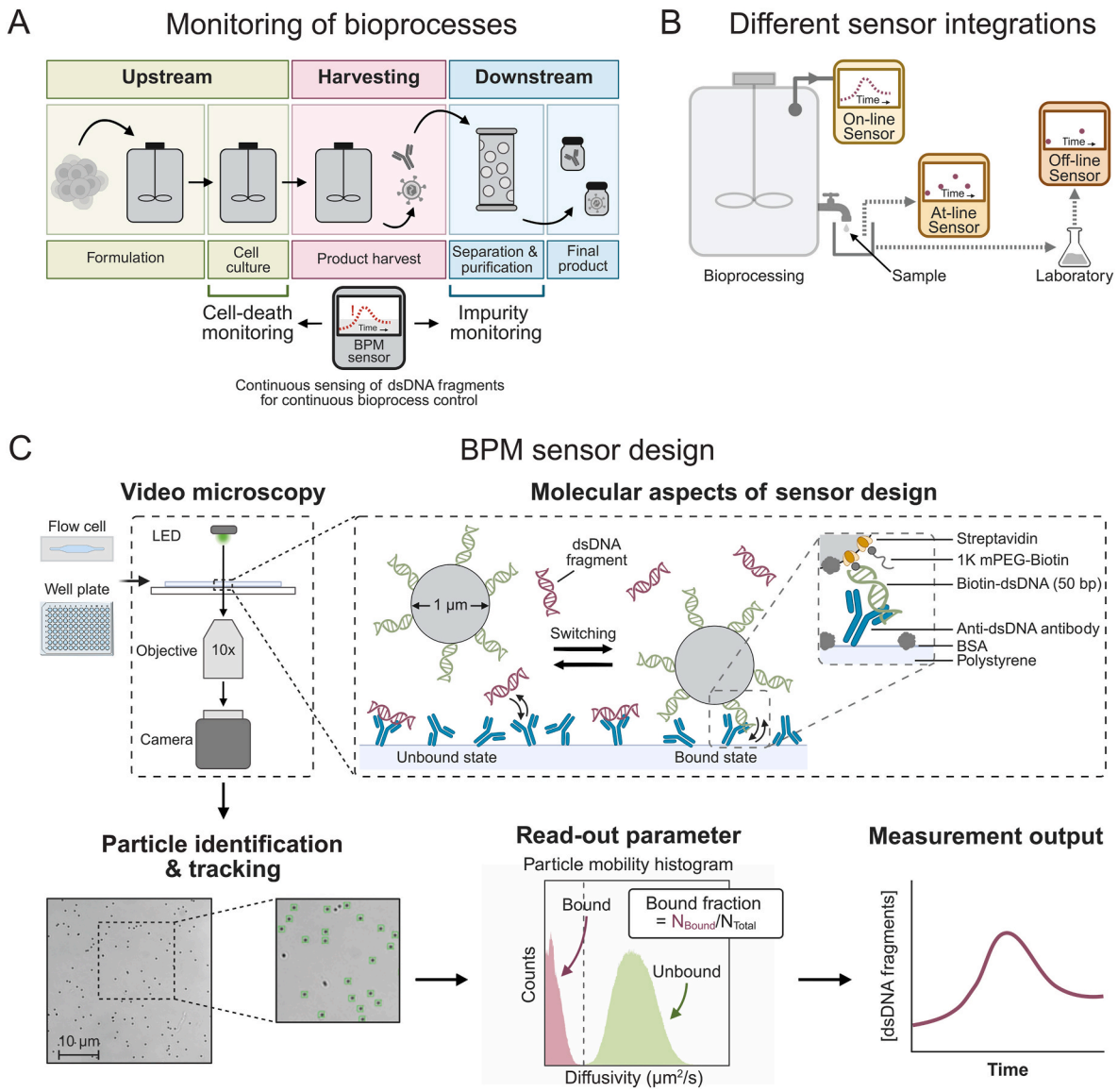

Fig. 1. Continuous biosensing of dsDNA fragments for bioprocess monitoring. (A) The three main steps in bioprocessing. Upstream processing for product formulation, cultivation, and development. Harvesting of the product when the desired quantity is reached. Downstream processing for extraction, purification, and quality control of the final product. (B) Sensor integrations into bioprocesses. In off-line monitoring, samples are taken from a bioreactor and then transported to and analyzed in an analytical laboratory. In at-line monitoring, samples are taken from a bioreactor and analyzed in a sensing system in the vicinity of the bioreactor. In on-line monitoring, all steps are automated: samples are automatically taken from a bioreactor and automatically transported to and measured in a sensing system. The aim of this work is to develop a continuous biosensing technology that, in the future, will be suited for off-line, at-line, and on-line measurements. (C) Sketch of the f-BPM dsDNA biosensor studied in this paper. Particles are functionalized with dsDNA fragments, and the sensing surface is functionalized with anti-dsDNA antibodies. Hundreds of particles are tracked by video microscopy, and their motion behavior depends on the dsDNA fragment concentration in the solution. Experiments in 96-well plates were used for developing the functionalization conditions, and sensors with microfluidic channels were used for performing continuous measurements. The diffusivity of the particles was determined from their time-dependent positions. The diffusivity value was used to determine the time-dependent state of every particle (bound or unbound). The bound fraction is the main readout parameter, defined as the ratio between the population of bound states and the total population of states over time. In a final application, the output of the sensor will be the dsDNA fragment concentration as a function of time.

study, the f-BPM sensor variant is used, due to its simpler fabrication process. In f-BPM, the particles stay close to the sensing surface due to the gravitational force that is caused by the higher mass density of the particles compared to the fluid. In a continuous sensing experiment, the particles remain inside the measurement chamber, as fluid samples are consecutively applied to the sensor with a relatively low flow speed.

The sensor of this study is designed with a competition format, with anti-dsDNA antibodies on the sensing surface and dsDNA fragments on the particles. The antibodies recognize the sugar-phosphate backbone of dsDNA, enabling sequence-independent binding to dsDNA (Pisetsky et al., 2021). In this study, we describe the sensor concept, show the feasibility of using anti-dsDNA antibodies in the sensor, demonstrate the reversibility of the biomolecular interactions in the sensor, and study the influence of the dsDNA fragment length. Finally, we show data on continuous monitoring of dsDNA fragments, evaluate sensor performance, and discuss the outlook of using real-time dsDNA sensing for both cell death monitoring in upstream processing and impurity monitoring in downstream processing.

2. Results and discussion

The results section is divided into two parts, with the first part discussing the monitoring of bioprocesses and the second part the experimental results of the sensor.

2.1. Monitoring of biomanufacturing processes

The three basic steps of bioprocessing are illustrated in Fig. 1A. The upstream part of a bioprocess involves the seeding and growth of cells in a bioreactor. Following cultivation, the product is harvested and subjected to downstream processing, which involves separation and purification to obtain a final product (Wasalathanthri et al., 2020). It is important to identify and monitor critical quality attributes (CQAs) in the processes to ensure consistent process performance and product quality. An interesting CQA for both up- and downstream processing is HCD (Grilo and Mantalaris, 2019), (Roch and Mandenius, 2016). In upstream processing, HCD levels can give information about cell status in the bioreactor since extracellular DNA appears in the medium upon death and lysis of cells (Grilo and Mantalaris, 2019). Furthermore, HCD is a host-related impurity that must be cleared from the final product (Wang et al., 2012). Therefore, monitoring HCD levels during downstream processing supports impurity clearance and enhances product safety.

Continuous monitoring refers to the continuous collection of measurement data from a process. A common strategy to perform continuous monitoring is by taking consecutive samples as a function of time and analyze each sample individually. As shown in Fig. 1B, measurements are performed off-line, at-line, or on-line, depending on the analytical measurement tool and its implementation. Off-line measurements are performed in a laboratory. At-line measurements are done locally on samples that are manually transferred to an analytical device. On-line measurements are automatically performed on samples that are automatically taken from the process. Nowadays, biomolecular measurements are mostly performed off-line and at-line, allowing a measurement frequency of a few samples per day (Claβen et al., 2017), (Lourenço et al., 2012). In contrast, on-line measurements are fully automatic, so can be performed at any time, and allow much higher measurement frequencies, facilitating enhanced process insight and control (Alford, 2006), (Reyes et al., 2022), (Veloso and Ferreira, 2017).

The biomolecular sensing technology studied in this paper aims to enable continuous measurements for at-line and on-line implementations. The basic concepts of the dsDNA f-BPM sensor are shown in Fig. 1C. The sensor is based on biofunctionalized particles with a diameter of 1 μm that interact with a biofunctionalized sensor surface (Buskermolen et al., 2022). The particles show diffusive Brownian motion while staying close to the surface, within a distance of about 1 μm, determined by the balance between Brownian motion and gravitational force (Buskermolen et al., 2022). The motions of hundreds of particles in a selected field of view (FOV) are recorded using a custom-made miniaturized microscope equipped with a high-speed camera. Particle tracking software is used to establish the positions of the particles from which the diffusivity (D) of every particle is determined as a function of time (Bergkamp et al., 2023). Histograms of measured diffusivities show two distinct populations, reflecting the bound and unbound states of the particles. Particle states with $D < 0.12\ \mu m^2/s$ are assigned as bound states, and particle states with $D > 0.12\ \mu m^2/s$ are assigned as unbound states.

The starting materials for the fabrication of the proof-of-concept sensor are a polystyrene surface and streptavidin-coated particles (ø1 μm MyOne Dynabeads). The surface is coated with anti-dsDNA antibodies via physisorption and blocked with bovine serum albumin (BSA) to reduce non-specific interactions. The particles are functionalized with biotinylated dsDNA of 50 base pairs and blocked with biotin-mPEG (polyethylene glycol) and BSA to suppress non-specific interactions with the surface. In this competitive sensor format, the particles have a high probability to bind to the antibodies on the surface when dsDNA fragments are not present in the solution, causing particles to often be in a bound state with low diffusivity. When dsDNA fragments are present in solution, they bind to the antibodies on the surface, thereby reducing the probability that particles can bind to the surface, leading to unbound states of the particles. The states of all particles in the FOV are monitored over time. The main readout parameter of the sensor is the bound fraction, which is defined as the ratio between the population of bound states and the total number of states, determined during a measurement duration for all tracked particles in the FOV.

2.2. Experimental results

The feasibility of the molecular design was tested by examining the functionalizations of the particle and surface, by screening binder concentrations, and by investigating the reversibility of the molecular interactions in 96-well plates (Fig. 2). The influence of the dsDNA fragment length on the sensor response was studied in flow cells to determine the dependence of the sensor response on the dsDNA fragment size (Fig. 3). Based on those results, continuous measurements were performed in sensors with one microfluidic channel to study the sensor response to varying concentrations over time (Figs. 4 and 5).

2.2.1. Sensor development: study of biofunctionalization densities and sensor reversibility

Experiments in well plates were used to establish the functionalization densities of particles and surface, as well as the reversibility of the bonds formed between particles and surface, as shown in Fig. 2. A direct assay (Fig. 2A) was used to evaluate the specificity of surface-immobilized anti-dsDNA antibodies for dsDNA-functionalized particles. The particles were functionalized by incubation with different biotin-dsDNA concentrations to vary the density of dsDNA on the particles. The wells were functionalized by incubation with different anti-dsDNA antibody concentrations to vary the density of antibodies on the well surface. Fig. 2A displays the bound fraction for bio-functionalized particles that were incubated on a well surface without dsDNA analyte in solution. An increase in both antibody and dsDNA densities led to higher bound fractions, confirming that the binding between particles and surface is driven by specific dsDNA–antibody interactions.

Next, to study the ability of the sensor to respond to different levels of dsDNA in solution, the analyte was pre-incubated for 30 min on the sensing surface before adding the particles. This reversed order—adding the sample before the particles—was used only in this experiment to investigate the concentration-dependent response of the sensor. Fig. 2B shows that for increasing dsDNA fragment concentrations in solution, the bound fraction decreases. This is attributed to dsDNA fragments

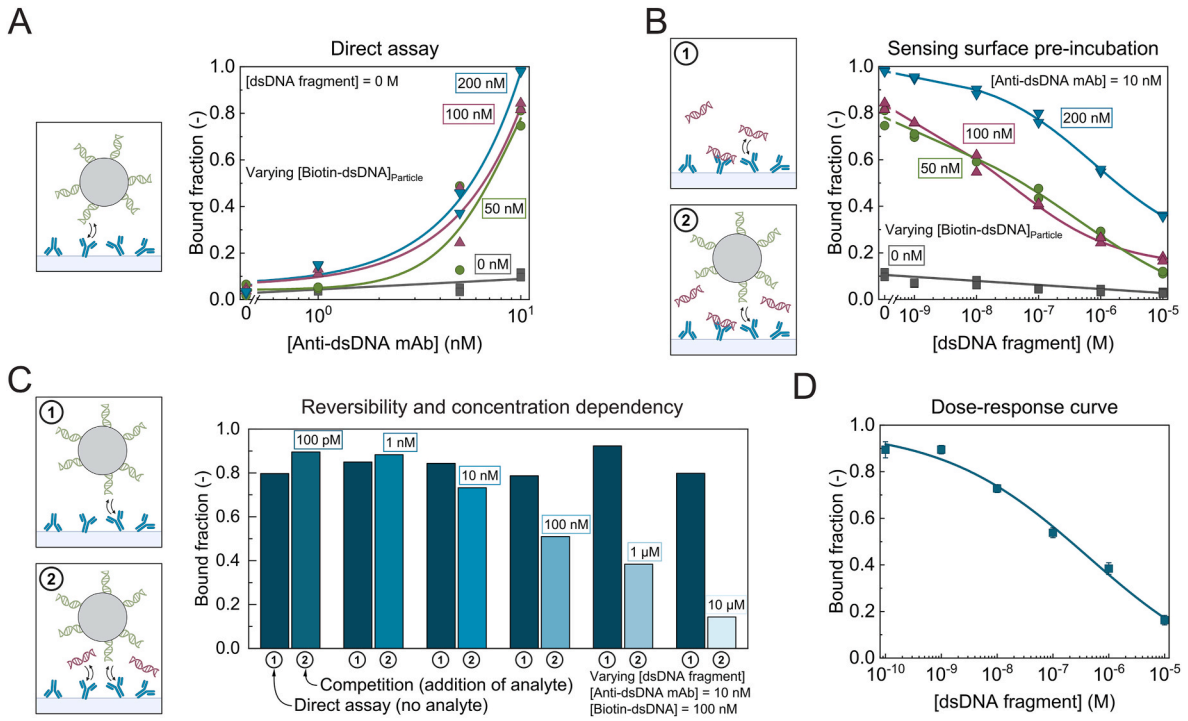

Fig. 2. Study of particle response and reversibility for different functionalizations of particles and surface, measured in 96-well plates. (A) Direct assay: particles functionalized with biotinylated dsDNA of 50 base pairs were added to a surface functionalized with anti-dsDNA antibodies. The bound fraction is shown as a function of the incubation concentration that was used to functionalize the surface. Curves are shown for different biotin-dsDNA incubation concentrations (0, 50, 100, 200 nM) to functionalize the particles. The data represents the bound fraction level for duplicate wells (n = 2). (B) The antibody-functionalized surface was pre-incubated with dsDNA fragments in solution, and thereafter, functionalized particles were added. The antibody incubation concentration for functionalizing the surface was kept constant at 10 nM. The curves show the bound fraction as a function of the dsDNA concentration in solution for particle functionalizations with different biotin-dsDNA incubation concentrations. The data represents the bound fraction level for duplicate wells (n = 2). (C) Functionalized particles were added to the functionalized surface without dsDNA in solution (direct assay, 20 min incubation). Next, dsDNA fragments (analyte) were added to the well to induce competition. The bars show the bound fraction of the direct assay (t = 0) and after the competition (t = 30 min). Experiments were performed with different dsDNA concentrations in solution. The decrease of the bound fraction for increasing dsDNA fragment concentrations indicates that the bonds between particles and surface are reversible and depend on the dsDNA concentration in solution. (D) The competition data in panel C is plotted as a dose-response curve. The data represents the mean ± standard deviation for the 3h measurements (see Fig. S2). In all panels, the lines are guides to the eye.

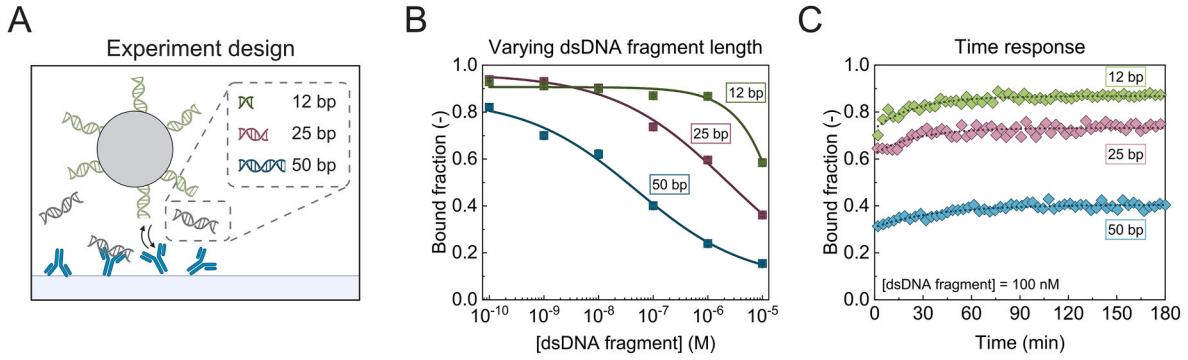

Fig. 3. Influence of dsDNA fragment length on the sensor response, measured in flow cells. (A) Sketch of the experimental design in which the dsDNA fragment lengths are varied between 12, 25, and 50 base pairs. The length of the biotin-dsDNA on the particles is kept constant at 50 base pairs. (B) The bound fraction as a function of dsDNA fragment concentration measured for the different fragment lengths. The data represents the mean ± standard deviation for the last 60 min of measurements (see Fig. S3). (C) Sensor response as a function of time for the different dsDNA fragment lengths at 100 nM concentration. In all panels, the lines are guides to the eye.

binding to the antibodies on the surface, which reduces the probability that particles become bound to the surface. The data show that the response of the assay can be tuned by varying the density of dsDNA coupled to the particles, keeping the antibody density on the surface constant.

Sensor reversibility is important for continuous monitoring applications. To investigate the reversibility of the interaction between the biotin-dsDNA on the particles and the anti-dsDNA antibodies on the surface, the particles were added first to the antibody-coated surface (Fig. 2C, as in the direct assay in Fig. 2A). Thereafter, the dsDNA analyte was added to the wells, which induced competition between the dsDNA in solution and the dsDNA on the particles for binding to the antibodies on the surface, leading to a drop in bound fraction. Fig. 2C shows decreasing bound fraction levels for increasing dsDNA fragment

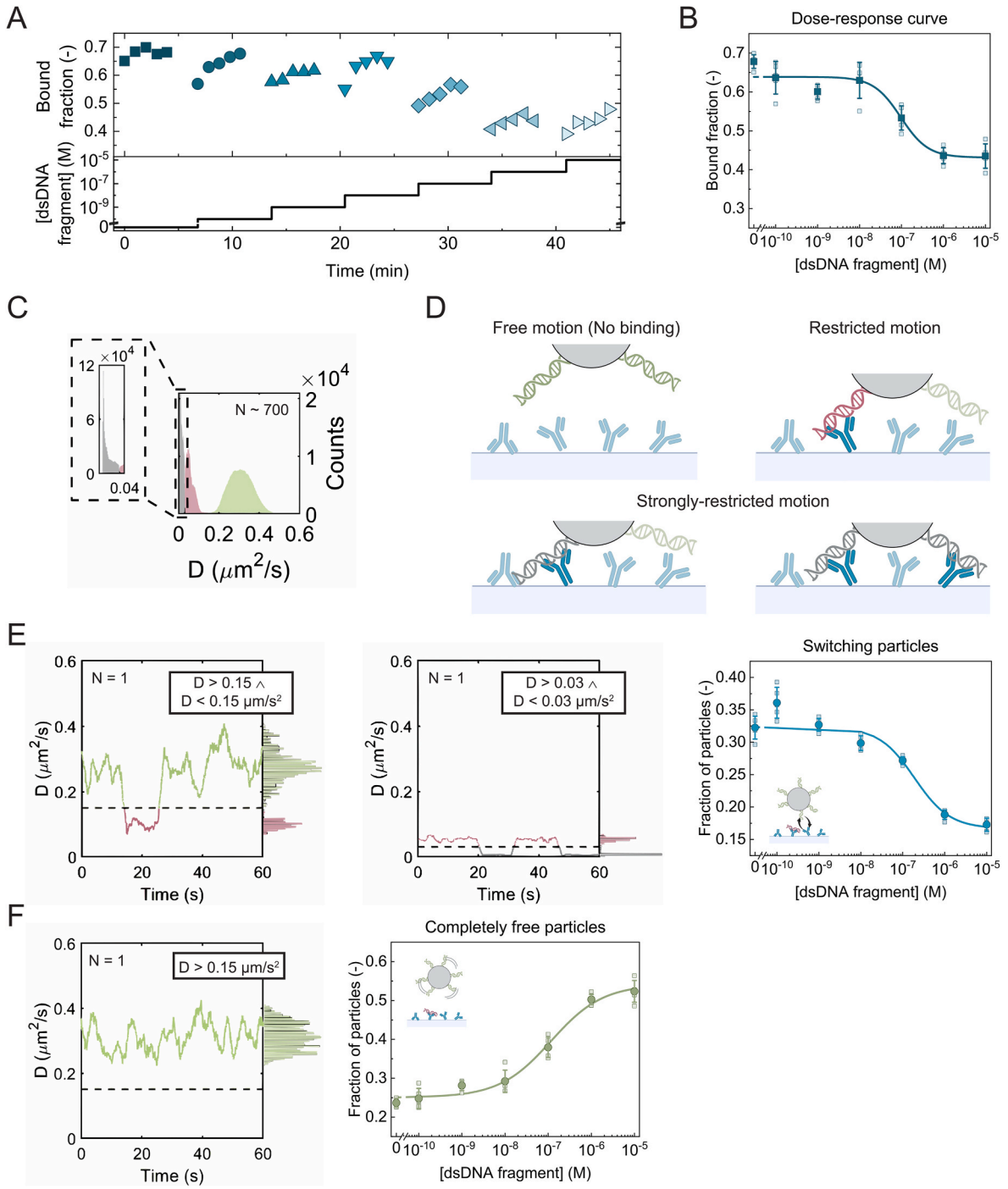

Fig. 4. Particle behavior measured in a flow cell with serial fluid replacements. (A) Bound fraction measured as a function of time (upper panel) for stepwise increasing dsDNA fragment concentrations (lower panel). (B) The data of (A) represented as a dose-response curve. The individual points and the average ± standard deviation are plotted for every dsDNA fragment concentration. (C) Diffusivity histogram of ~700 particles measured after injection of 100 nM dsDNA in the experiment of panel A. Three different groups can be distinguished: diffusivity below 0.03 μm/s^2 (grey), diffusivity between 0.03 and 0.15 μm/s^2 (red), and diffusivity above 0.15 μm/s^2(green). These groups represent particles with strongly-restricted motion, restricted motion, and free motion, respectively. (D) Possible interpretations of the three groups. No bond results in free motion. Single antibody-dsDNA bonds may result in restricted motion. Multiple antibody-dsDNA bonds may result in strongly-restricted motion. (E) Particles that show switching behavior. Left: A particle that switches between free and restricted motion. Middle: A particle that switches between restricted and strongly-restricted motion. The dashed lines in the diffusion time traces represent the thresholds. Right: The fraction of all particles showing switching behavior plotted as a function of dsDNA concentration. The data represents both the individual data points and the mean ± standard deviation for the five measurements per dsDNA fragment concentration. (F) Left: Diffusion time trace of a particle that does not show any binding. The dashed line represents the threshold. Right: The fraction of all particles that do not show any binding plotted as a function of dsDNA concentration. The data represents the mean ± standard deviation for the five measurements per dsDNA fragment concentration as well as the individual data points. In all panels, the lines are guides to the eye.

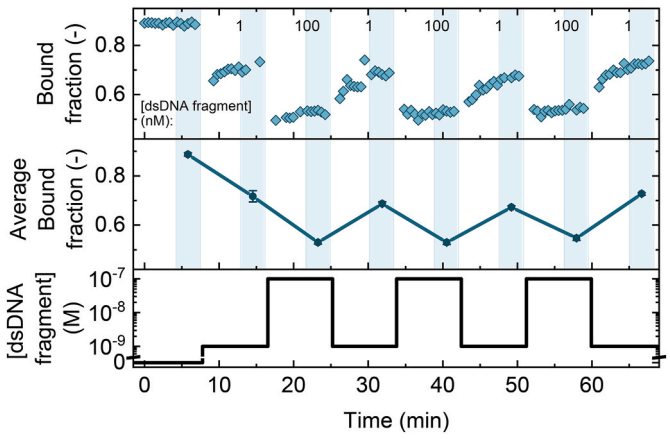

Fig. 5. Demonstration of continuous monitoring of short dsDNA fragments, measured in a flow cell. Samples with dsDNA fragment concentrations of 1 and 100 nM were added in alternating order (bottom panel), and the response in bound fraction was measured (top panel, measurements of 15 s each, measured 15 times for every concentration), both on the same time scale. The average bound fraction and the standard deviation (mid panel) were calculated using the last five datapoints per sample (indicated with the lightblue bars). The bound fraction shows an alternating trend in response to alternating dsDNA fragment concentrations.

concentrations, demonstrating that the bonds between dsDNA on the particles and the antibodies are reversible and that the competition is concentration dependent. The sensor responds within 5 min to the addition of analyte and shows a stable signal over time (Fig. S2). The dose-response curve based on the data in Fig. 2C after the addition of dsDNA fragments is plotted in Fig. 2D, confirming the signal dependency on dsDNA fragment concentration.

All the above experiments were performed in well plates to assess the feasibility of the competitive sensor's molecular design. The results prove that the sensor responds to different dsDNA concentrations through reversible interactions. However, well plates are not suitable for fluid exchange and flow, which is needed for continuous sensing experiments. Therefore, in the next sections, the sensor behavior is studied in microfluidic flow cells.

2.2.2. *Sensor response to different dsDNA fragment lengths*

In the previous section, we explored the feasibility of the competitive dsDNA sensor in well plate experiments with 50 bp dsDNA. Here, flow cell experiments are performed, first focusing on the influence of the length of the dsDNA fragments on the sensor response. Extracellular dsDNA appears in biomanufacturing processes with different lengths, due to fragmentation in the cell lysis process and due to mechanical shear forces in the bioreactor. This raises the question of how the sensor response depends on fragment length, and the related question how the anti-dsDNA antibodies interact with dsDNA. Anti-dsDNA antibodies bind to DNA by monogamous bivalency, a mechanism where both paratopes bind to specific parts on the same DNA strand (Pisetsky et al., 2022). Each paratope of the antibody binds to approximately three base pairs of dsDNA with a relatively weak affinity. A more stable bond arises when both paratopes of the antibody simultaneously bind to a single piece of dsDNA. To enable bivalent binding, the dsDNA fragment must span the inter-paratope distance, requiring a minimum length of approximately 16 base pairs (Abcam). Therefore, it is interesting to know how the antibody-based BPM sensor responds to dsDNA fragments with a length of several tens of base pairs.

The BPM sensor was exposed to dsDNA fragments with lengths of 12, 25, and 50 base pairs, as shown in Fig. 3A. The dose-response curves in Fig. 3B shift to the left for increasing fragment lengths, indicating that the sensor is more sensitive to the fragments with longer lengths. To get a similar sensor response as for the 50 base pair fragments, the concentration of the 25 base pair fragments needs to be 30-fold higher, and for the 12 base pair fragments 250-fold higher, compared to the 50 base pair fragments. The observed increase in antibody binding with longer dsDNA fragments can be caused by a combination of several effects: the need for sufficient DNA length to enable monogamous bivalency, reduced steric hindrance as longer dsDNA fragments are less rigid, and/or enhanced electrostatic interactions for longer fragments that could improve sensor sensitivity. Geometrically, longer fragments have a higher probability than shorter fragments of binding to two paratopes on a single antibody, or to two paratopes on two different antibodies. The present data is not sufficient to draw conclusions about the precise nature of the biomolecular binding between particles and sensing surface. This can be studied in more detail by analyzing distribution functions of particle bound-state lifetimes (Visser et al., 2018). Establishing such functions requires long particle observation times to collect sufficient statistics, which is more suited for t-BPM than for f-BPM experiments; this is a topic for further research.

Fig. 3C shows the time evolution of the signals measured after exposure to the different fragment lengths. The fragment-induced sensor response is visible within a minute after injection of the dsDNA containing solution into the flow cell, followed by a slow increase of the signal on a timescale of hours, which is independent of the dsDNA fragment length. The fast response is attributed to specific interactions between antibodies and dsDNA. The slow drift may be caused by non-specific interactions between particle and sensing surface, or by specific interactions that occur on long timescales, e.g. related to molecular heterogeneities in the sensor (Vu et al., 2025).

2.2.3. *Characterization of sensor response with sequential fluid applications*

In a continuous f-BPM biosensor, hundreds of individual particles are continuously monitored, and their motion behaviors are related to the concentration of analyte in solution. In this section, sequential dsDNA fragment concentrations are injected in increasing order into a flow cell, to study the sensor response and particle behavior, see Fig. 4.

First, the sensor response, i.e., the bound fraction as a function of increasing dsDNA fragment concentrations, is determined to confirm that single flow cells can be used for continuous monitoring experiments. Fig. 4A displays the time-resolved bound fraction (top panel) alongside the corresponding dsDNA fragment concentrations introduced (bottom panel). With increasing dsDNA fragment concentration, the bound fraction decreases due to the competitive binding mechanism of the sensor. The fragment-induced sensor response is visible within a minute after injection of the dsDNA-containing solution into the flow cell, followed by a slow increase of the signal on a longer timescale. Potential origins of the slow signal increase are not yet clear. The increase may be caused by flow-induced dissociations of bonds between particle and surface that slowly re-equilibrate, or by slow non-specific or specific interactions between particle and surface; this is to be further investigated in follow-up research. Fig. 4B shows the dose-response curve based on the data in Fig. 4A, visualizing the signal decrease for increasing analyte concentrations.

To understand the origin of the sensor response, histograms of motion characteristics can help to gain insights into the nature of the binding between particle and surface. Fig. 4C visualizes a diffusivity histogram of approximately 700 particles measured after injection of 100 nM dsDNA in the experiment of panel A. The data shows three groups: motion states with low diffusivity ($D < 0.03$ μm^2/s, strongly-restricted motion, grey), motion states with medium diffusivity (0.03 μm^2/s $< D <$ 0.15 μm^2/s, restricted motion, red), and states with free motion ($D >$ 0.15 μm^2/s, green). Fig. 4D illustrates the hypothesized binding configurations corresponding to each motion state. Strongly-restricted motion likely results from multiple antibody-dsDNA interactions, while single bonds yield restricted motion, and unbound particles exhibit free diffusion.

The motion groups observed in Fig. 4C allow one to study if particles switch reversibly between motion states. Two motion time traces of

particles with switching activity are displayed in Fig. 4E: a particle that shows switching behavior between free and restricted motion (left) and a particle that switches between restricted and strongly-restricted motion (middle). The motion time traces of all particles can be analyzed at different dsDNA concentrations to establish dose-response relationships. The right panel in Fig. 4E shows the fraction of particles with switching behavior, plotted as a function of dsDNA concentration. The fraction decreases with increasing dsDNA fragment concentration, likely due to antibody saturation on the surface, resulting in more free particles. Fig. 4F supports this interpretation by showing a non-interacting particle (left) and a corresponding increase in the fraction of non-interacting particles with rising dsDNA concentration (right). The fraction increases as a function of dsDNA fragment concentration due to the blocking of the antibodies on the surface. Interestingly, the dose-response curves for bound fraction (4B), fraction of switching particles (4E), and fraction of non-interacting particles (4F) all show a maximum slope at around 100 nM, suggesting that this might be the magnitude of the equilibrium dissociation constant of the interaction between the anti-dsDNA antibodies on the surface and the 50 base pair dsDNA fragments in solution.

2.2.4. Feasibility of continuous monitoring studied with alternating dsDNA fragment concentrations

The previous sections demonstrated that the interaction between the anti-dsDNA antibodies on the sensing surface and the dsDNA on the particles is modulated by the dsDNA fragment concentration in solution. The ability of the sensor to reversibly respond to both increasing and decreasing dsDNA fragment concentrations is studied in this section. Fig. 5 presents the bound fraction signal (top panel) in response to sequentially applied dsDNA fragment concentrations (bottom panel). The middle panel shows the average bound fraction of the last five data points in each interval in the upper panel.

The injections of 100 nM dsDNA give sensor responses within a minute, followed by stable signal values. This shows that the binding of dsDNA in solution to the antibodies and the subsequent release of particles from the surface are fast processes. In contrast, the 1 nM dsDNA injections cause gradual increases of bound fraction values, which indicates that the release of dsDNA from the antibodies is a relatively slow process. The average bound fraction curve shows that the sensor responds reversibly to the modulation of dsDNA concentration. This demonstrates that the sensor is reversible and is suited in principle for the continuous monitoring of increasing as well as decreasing dsDNA fragment concentrations.

3. Conclusion and outlook

We demonstrated that continuous monitoring of dsDNA fragments in nanomolar to micromolar concentrations is achievable using biosensing by free particle motion (f-BPM) with a competitive sensor design, having anti-dsDNA antibodies on the sensing surface and dsDNA on the particles. The sensor is independent of the dsDNA sequence as the antibodies target the sugar-phosphate backbone of DNA. Furthermore, the sensor can detect dsDNA fragments of varying sizes and was demonstrated to be reversible, showing response to both increasing and alternating dsDNA fragment concentration profiles. The ability to continuously monitor dsDNA without consuming reagents is a unique property of this sensor.

The presented results are a first step towards developing a continuous HCD sensing system for bioprocess monitoring (Roch and Mandenius, 2016), (Hu et al., 2021). Overview papers have discussed comparisons between spectroscopic, chromatographic, and biosensing techniques for achieving bioprocess analysis (Sathiyapriyan et al., 2025), (Rolinger et al., 2020). Spectroscopic techniques fall behind chromatographic techniques in terms of specificity, while chromatographic techniques are demanding on sample preparation procedures. Biosensing techniques give opportunities to fill in the gaps, by potentially combining high specificity with fast measurements and simple sample preparations.

In the described BPM sensor, the anti-dsDNA antibodies are the molecules that give specificity towards the dsDNA targets. The proof-of-concept sensor was studied with TBS buffer. In follow-up research, it will be important to study the properties of the sensor in solutions relevant for process control, e.g. in cell growth medium for upstream processing, and in extraction and purification buffers for downstream processing. We foresee diverse applications for continuous dsDNA sensors, targeting different sample matrices and different dsDNA concentrations (high nanomolar to picomolar). However, many research questions still need to be addressed. Further research should address topics such as fragment length dependence, sample pretreatment, sensor sensitivity, sensor kinetics, and long-term monitoring capabilities.

This study focused on detecting 50 base pair dsDNA fragments at nanomolar to micromolar concentrations. In bioprocessing, fragment lengths can vary from around a hundred base pairs up to several hundreds of kilo base pairs (Matassov et al., 2004), (Rolinger et al., 2020). Monitoring fragments equal to or shorter than a typical gene (~200 base pairs) is especially relevant for downstream processing (U.S. Food and Drug Administration (FDA) and & Center for Biologics Evaluation and Research (CBER), 2010). Therefore, in follow-up work, the sensor response to dsDNA fragments with diverse sizes will be studied in buffer solutions and bioprocessing matrices. It is also relevant to investigate sample pre-treatment protocols, such as ultrasonic treatments to change and control DNA fragment sizes (Elsner and Lindblad, 1989). Furthermore, building on this work, BPM sensors can be designed with higher detection sensitivities (Rolinger et al., 2020), (Butler et al., 2009), potentially by using BPM sensor designs with molecular sandwich formats (Michielsen et al., 2025).

This paper studied the feasibility of continuous dsDNA monitoring in a competition-based f-BPM flow cell sensor. Continuous measurements with f-BPM sensors are limited to low flow speeds, to minimize flow-induced losses of particles. The fabrication of dsDNA sensors with a tether molecule between particle and surface (t-BPM) (Visser et al., 2018) will allow for fluid replacements with higher flow velocities and measurements over longer durations to investigate topics such as sensor kinetics, measurement precision, limits of quantification, and measurement accuracy (Michielsen et al., 2025), (Lubken et al., 2024). Finally, it will be interesting to demonstrate the sensors with automated fluid control systems to achieve automated, continuous sampling-and-sensing for HCD-based bioprocess monitoring and control.

4. Materials

Nunc maxisorp clear flat bottom 96-well plates (Invitrogen) and Dynabeads® MyOne™ C1 Streptavidin 1 μm (Invitrogen, 10 mg/mL) were obtained from ThermoFisher Scientific. The particles consist of iron oxide cores with a polystyrene shell that is coated with streptavidin. Tris Buffered Saline (TBS) tablets, sodium carbonate, sodium bicarbonate (anhydrous), and bovine serum albumin (BSA) were ordered at Sigma-Aldrich. The dsDNA and biotin-dsDNA fragments were custom designed and ordered at Integrated DNA Technologies. The specific sequences can be found in the Supplementary (S2). Anti-dsDNA antibody [35I9 DNA] (1 mg/mL) was purchased from Abcam, and mPEG-biotin (MW 1 kDa) was obtained from Nanocs (USA). Polystyrene sheets (300 mm x 300 mm, thickness 1.2 mm) were purchased from Goodfellow Corporation (ST31-SH-000120) and laser-cut to 25 mm × 75 mm. Custom-made flow cell stickers with a chamber height of 250 μm, an internal volume of ~20 μL, and six cells per sticker were purchased from Grace Biolabs (USA).

4.1. Particle preparation

2 μL of the streptavidin coated particles were incubated with 2 μL of 0, 50, 100 or 200 nM biotin-dsDNA on a rotary fin for 45 min. The particles were blocked with 40 μL 100 μM biotin-mPEG for 20 min. Next,

the particles were washed 3 times with 200 μL TBS on a magnetic rack. The particles were resuspended in 200 μL TBS containing 1 % BSA and incubated on a rotary fin for 60 min. Finally, the particles were sonicated 10 pulses with an amplitude of 70 % and 0.5 s duty cycle (Hielscher UIS250V, Ultrasound Technology) and diluted in TBS 12.5 times for the direct assay and surface incubation, 20 times for the reversibility test, and 30 times for flow cell experiments.

4.2. 96-Well plate experiments

Anti-dsDNA antibodies were diluted to 1, 5, or 10 nM in 0.1 M sodium carbonate-bicarbonate buffer (pH 10). 50 μL of the antibodies were added to the well plate and incubated overnight at 4 °C. The solution was removed from all the wells before adding 50 μL TBS with 1 % BSA, which was incubated for 60 min at room temperature (RT). Again, all the wells were emptied before adding the particles and analyte solution. For the direct assay and surface incubation, 25 μL of TBS or dsDNA fragment solution were added to specific wells and incubated for 30 min. The dsDNA fragment was diluted in TBS to 2 nM–20 μM (10 times serial dilution). Afterwards, 25 μL of particles were added, and measurements were started after 10 min of incubation and particles sedimentation. The particle motion was recorded for 12 s in each well. The whole well plate was measured 20 times. For the reversibility assay, 40 μL of particles were added and incubated for 20 min. Subsequently, all wells were scanned once for 12 s to determine the bound fraction. Then, 10 μL of TBS or dsDNA fragment solutions in concentrations from 5 to 50 nM (10 times serial dilution) were added to the specific wells and measurements were started immediately. The particle motion was again recorded for 12 s per well, and the whole plate was scanned 100 times.

4.3. Flow cell experiments

Custom-made flow cell stickers were attached to a polystyrene slide. All solutions were manually added in a volume of 40 μL to the flow cell, except for the dsDNA fragment solutions, which were injected in a volume of 60 μL. First, the antibodies (diluted in 0.1 M sodium carbonate-bicarbonate buffer at pH 10) were added to the flow cell and incubated for 2 h at RT, followed by addition of TBS with 1 % BSA, which was incubated for another hour. Next, the particles were added to the flow cell and were left to sediment for approximately 15 min. For the separate flow cell experiments, dsDNA fragment concentrations ranging from 100 pM to 10 μM (10 times serial dilution) were added to separate flow cells, followed by immediately starting the measurement. The particle motion was recorded in 12 s periods, and all flow cells were measured 100 times over 3 h by scanning the slide with respect to the optical imaging system. During the incubation and measuring period, the in- and outlets were sealed with tape.

For the serial fluid replacement, dsDNA fragment concentrations ranging from 100 pM to 10 μM (10 times serial dilution) were added sequentially to a flow cell. For each concentration, particles were tracked either for 5 min in five 1-min blocks (for increasing concentrations) or for approximately 8 min in fifteen 15-s blocks (for alternating concentrations). The 1-min measurements for increasing concentrations allow analysis of particle behavior within the sensor, while the shorter 15-s measurements for alternating concentrations provide higher temporal resolution to capture the bound fraction profile. The duration of the measurement block determines the statistics of the particle diffusivity histograms and, therefore, the precision of the bound fraction determination.

4.4. Data acquisition and processing

All measurements were performed using a custom-built microscope with a motorized XY stage (ASR series, 100 mm × 120 mm travel; Zaber Technologies Inc.). The particles were visualized using brightfield illumination, i.e., with a green LED (12V, 3 mm), 10x magnification (10x DIN Achromatic Finite Intl Standard Objective, from Edmund Optics), and a high-speed camera (FLIR Blackfly S BFS-U3-31S4M or FLIR Grasshopper 3 GS3-U3-32S4M-C, from Edmund Optics) with a field-of-view of 706 × 530 μm and an effective pixel size of 0.587 × 0.587 μm. The particles were tracked at a frame rate of 60 Hz. A miniature linear actuator (Zaber T-LA13A) was built in the microscope to autofocus between measurement blocks. MATLAB was used to control the custom-built microscope setup. Dedicated particle tracking software described by Bergkamp et al. (2023) was utilized to track the position of the particles in real-time, applying two-dimensional phasor-based localization (Martens et al., 2018). The diffusivity of the particles was determined from their positions, and a diffusivity threshold of 0.12 $\mu m^2/s$ was used to distinguish unbound from bound states. The bound fraction was used as output parameter and is defined as the ratio between the population of bound states and the total population of states over time.

4.5. Particle classification and behavior determination

The particles were classified in 4 different groups based on their motion behavior during the 1 min measurement time. The 4 groups are: 1) free particles with diffusivities above 0.15 $\mu m^2/s$, 2) switching particles with diffusivities crossing the set thresholds at either 0.03 $\mu m^2/s$ or 0.15 $\mu m^2/s$ or both, 3) restricted particles with diffusivities between 0.03 and 0.15 $\mu m^2/s$, and 4) strongly-restricted particles with diffusivities lower than 0.03 $\mu m^2/s$. The amount of particles in a group is compared to the total amount of particles to determine the fraction of particles in that specific group.

CRediT authorship contribution statement

Selina A.J. Janssen: Writing – review & editing, Writing – original draft, Visualization, Methodology, Investigation, Conceptualization. **Arthur M. de Jong:** Writing – review & editing, Supervision, Methodology, Conceptualization. **Menno W.J. Prins:** Writing – review & editing, Supervision, Methodology, Conceptualization.

Declaration of competing interest

The authors do not declare a competing interest.

Acknowledgements

We thank Stijn Haenen for building the compact microscope setups. We thank Max Bergkamp for providing the real-time particle tracking algorithms. Part of this work was funded by the Netherlands National Growth Fund Programme NxtGen Hightech. Part of this work was supported by the NWO KIEM HighTech program.

Appendix A. Supplementary data

Supplementary data to this article can be found online at https://doi.org/10.1016/j.bios.2025.117808.

Data availability

Data will be made available on request.

References

Abcam. (n.d.). *Anti-ds DNA antibody [35I9 DNA] – BSA and azide free* [product datasheet]. Retrieved February 11, 2025, from https://doc.abcam.com/datasheets/active/ab27156/en-us/ds-dna-antibody-35i9-dna-bsa-and-azide-free-ab27156.pdf.

Alford, J.S., 2006. Bioprocess control: advances and challenges. Comput. Chem. Eng. 30 (10–12), 1464–1475. https://doi.org/10.1016/J.COMPCHEMENG.2006.05.039.

Becker, T., Hitzmann, B., Muffler, K., Pörtner, R., Reardon, K.F., Stahl, F., Ulber, R., 2006. Future aspects of bioprocess monitoring. In: Ulber, R., Sell, D. (Eds.), White Biotechnology, 105. Springer, pp. 249–293. https://doi.org/10.1007/10_2006_036.

Bergkamp, M.H., Cajigas, S., IJzendoorn, L. J. van, Prins, M.W.J., 2023. High-throughput single-molecule sensors: how can the signals be analyzed in real time for achieving real-time continuous biosensing? ACS Sens. 8 (6), 2271–2281. https://doi.org/10.1021/ACSSENSORS.3C00245.

Buskermolen, A.D., Lin, Y.-T., van Smeden, L., van Haaften, R.B., Yan, J., Sergelen, K., de Jong, A.M., Prins, M.W.J., 2022. Continuous biomarker monitoring with single molecule resolution by measuring free particle motion. Nat. Commun. 13, 6052. https://doi.org/10.1038/s41467-022-33487-3.

Butler, M.D., Kluck, B., Bentley, T., 2009. DNA spike studies for demonstrating improved clearance on chromatographic media. J. Chromatogr. A 1216 (41), 6938–6945. https://doi.org/10.1016/J.CHROMA.2009.08.049.

Claßen, J., Aupert, F., Reardon, K.F., Solle, D., Scheper, T., 2017. Spectroscopic sensors for in-line bioprocess monitoring in research and pharmaceutical industrial application. Anal. Bioanal. Chem. 409 (3), 651–666. https://doi.org/10.1007/S00216-016-0068-X/FIGURES/2.

Elsner, H.I., Lindblad, E.B., 1989. Ultrasonic degradation of DNA. DNA Cell Biol. 8 (10), 697–701. https://doi.org/10.1089/DNA.1989.8.697.

Glindkamp, A., Riechers, D., Rehbock, C., Hitzmann, B., Scheper, T., Reardon, K.F., 2009. Sensors in disposable bioreactors: status and trends. In: Scheper, T. (Ed.), Advances in Biochemical Engineering/Biotechnology, 115. Springer, pp. 1–44. https://doi.org/10.1007/10_2009_10.

Grilo, A.L., Mantalaris, A., 2019. Apoptosis: a mammalian cell bioprocessing perspective. Biotechnol. Adv. 37 (3), 459–475. https://doi.org/10.1016/J.BIOTECHADV.2019.02.012.

Hu, X.M., Li, Z.X., Lin, R.H., Shan, J.Q., Yu, Q.W., Wang, R.X., Liao, L.S., Yan, W.T., Wang, Z., Shang, L., Huang, Y., Zhang, Q., Xiong, K., 2021. Guidelines for regulated cell death assays: a systematic summary, A categorical comparison, A prospective. Front. Cell Dev. Biol. 9, 634690. https://doi.org/10.3389/FCELL.2021.634690/BIBTEX.

Ikeda, Y., Iwakiri, S., Yoshimori, T., 2009. Development and characterization of a novel host cell DNA assay using ultra-sensitive fluorescent nucleic acid stain “PicoGreen.”. J. Pharmaceut. Biomed. Anal. 49 (4), 997–1002. https://doi.org/10.1016/J.JPBA.2009.01.022.

Isoko, K., Cordiner, J.L., Kis, Z., Moghadam, P.Z., 2024. Bioprocessing 4.0: a pragmatic review and future perspectives. Digit. Discov. 3 (9), 1662–1681. https://doi.org/10.1039/D4DD00127C.

Lauro, M.L., Bowman, A.M., Smith, J.P., Gaye, S.N., Acevedo-Skrip, J., DePhillips, P.A., Loughney, J.W., 2023. Overcoming biopharmaceutical interferents for quantitation of host cell DNA using an automated, high-throughput methodology. AAPS J. 25 (1), 10. https://doi.org/10.1208/s12248-022-00764-4.

Lourenço, N.D., Lopes, J.A., Almeida, C.F., Sarraguça, M.C., Pinheiro, H.M., 2012. Bioreactor monitoring with spectroscopy and chemometrics: a review. Anal. Bioanal. Chem. 404 (4), 1211–1237. https://doi.org/10.1007/S00216-012-6073-9/TABLES/6.

Lubken, R.M., Lin, Y.-T., Haenen, S.R.R., Bergkamp, M.H., Yan, J., Nommensen, P.A., Prins, M.W.J., 2024. Continuous biosensor based on particle motion: how does the concentration measurement precision depend on time scale? ACS Sens. 9 (10), 4924–4933. https://doi.org/10.1021/ACSSENSORS.4C01586.

Martens, K.J.A., Bader, A.N., Baas, S., Rieger, B., Hohlbein, J., 2018. Phasor based single-molecule localization microscopy in 3D (pSMLM-3D): an algorithm for MHz localization rates using standard CPUs. J. Chem. Phys. 148 (12), 123311. https://doi.org/10.1063/1.5005899.

Matassov, D., Kagan, T., Leblanc, J., Sikorska, M., Zakeri, Z., 2004. Measurement of apoptosis by DNA fragmentation. In: Brady, H.J.M. (Ed.), Apoptosis Methods and Protocols, 282. Humana Press, pp. 1–17. https://doi.org/10.1385/1-59259-812-9:001.

Michielsen, C.M.S., Yan, J., Lin, Y.-T., Bergkamp, M.H., Haenen, S.R.R., Lubken, R.M., Grawe, A., Swietlikowska, A., de Jong, A.M., Prins, M.W.J., 2025. Reversible sandwich-based particle nanoswitch for continuous protein monitoring at picomolar concentrations with automated calibration. bioRxiv. https://doi.org/10.1101/2025.06.13.659459 [Preprint].

Nissom, P.M., 2007. Specific detection of residual CHO host cell DNA by real-time PCR. Biologicals 35 (3), 211–215. https://doi.org/10.1016/J.BIOLOGICALS.2006.09.001.

Pisetsky, D.S., Shaffer, R., Armstrong, D.D., Spencer, D.M., 2021. The interaction of anti-DNA antibodies with DNA antigen: evidence for hysteresis for high avidity binding. Clin. Immunol. 231, 108848. https://doi.org/10.1016/J.CLIM.2021.108848.

Pisetsky, D.S., Garza Reyna, A., Belina, M.E., Spencer, D.M., 2022. The interaction of anti-DNA antibodies with DNA: evidence for unconventional binding mechanisms. Int. J. Mol. Sci. 23 (9), 5227. https://doi.org/10.3390/ijms23095227.

Rathore, A.S., 2016. Quality by design (QbD)-Based process development for purification of a biotherapeutic. Trends Biotechnol. 34 (5), 358–370. https://doi.org/10.1016/J.TIBTECH.2016.01.003.

Reyes, S.J., Durocher, Y., Pham, P.L., Henry, O., 2022. Modern sensor tools and techniques for monitoring, controlling, and improving cell culture processes. Processes 10 (2), 189. https://doi.org/10.3390/pr10020189.

Roch, P., Mandenius, C.F., 2016. On-line monitoring of downstream bioprocesses. Curr. Opin. Chem. Eng. 14, 112–120. https://doi.org/10.1016/J.COCHE.2016.09.007.

Rolinger, L., Rüdt, M., Hubbuch, J., 2020. A critical review of recent trends, and a future perspective of optical spectroscopy as PAT in biopharmaceutical downstream processing. Anal. Bioanal. Chem. 412 (9), 2047–2064. https://doi.org/10.1007/S00216-020-02407-Z.

Sathiyapriyan, P., Mukherjee, S., Vogel, T., Essen, L., Boerema, D., Vey, M., Kalina, U., 2025. Current PAT landscape in the downstream processing of biopharmaceuticals. Analyt. Sci. Adv. 6 (1), e70013. https://doi.org/10.1002/ANSA.70013.

U.S. Food and Drug Administration (FDA), & Center for Biologics Evaluation and Research (CBER), 2010. Guidance for industry: characterization and qualification of cell substrates and other biological materials used in the production of viral vaccines for infectious disease indications. https://www.fda.gov/media/78428/download.

Veloso, A.C., Ferreira, E.C., 2017. Online analysis for industrial bioprocesses: broth analysis. In: Current Developments in Biotechnology and Bioengineering: Bioprocesses, Bioreactors and Controls. Elsevier, pp. 679–704. https://doi.org/10.1016/B978-0-444-63663-8.00023-9.

Visser, E.W.A., Yan, J., van IJzendoorn, L.J., Prins, M.W.J., 2018. Continuous biomarker monitoring by particle mobility sensing with single molecule resolution. Nat. Commun. 9, 2541. https://doi.org/10.1038/s41467-018-04802-8.

Vu, C., Yan, J., de Jong, A.M., Prins, M.W.J., 2025. How highly heterogeneous sensors with single-molecule resolution can result in robust continuous monitoring over long time spans. Adv. Sci. 12 (7), 2412181. https://doi.org/10.1002/advs.202412181.

Wang, X., Morgan, D.M., Wang, G., Mozier, N.M., 2012. Residual DNA analysis in biologics development: review of measurement and quantitation technologies and future directions. Biotechnol. Bioeng. 109 (2), 307–317. https://doi.org/10.1002/BIT.23343.

Wasalathanthri, D.P., Rehmann, M.S., Song, Y., Gu, Y., Mi, L., Shao, C., Chemmalil, L., Lee, J., Ghose, S., Borys, M.C., Ding, J., Li, Z.J., 2020. Technology outlook for real-time quality attribute and process parameter monitoring in biopharmaceutical development—A review. Biotechnol. Bioeng. 117 (10), 3182–3198. https://doi.org/10.1002/bit.27461.

World Health Organization (WHO), & WHO Expert Committee on Biological Standardization, 2014. *WHO Expert Committee on Biological Standardization: Sixty-Fourth Report* (WHO Technical Report Series, No. 987). World Health Organization. https://apps.who.int/iris/handle/10665/129494.

Wu, S., Ketcham, S.A., Corredor, C.C., Both, D., Drennen, J.K., Anderson, C.A., 2023. Capacitance spectroscopy enables real-time monitoring of early cell death in mammalian cell culture. Biotechnol. J. 18 (3), 2200231. https://doi.org/10.1002/BIOT.202200231.

Zhang, Y.H.P., Sun, J., Ma, Y., 2017. Biomanufacturing: history and perspective. J. Ind. Microbiol. Biotechnol. 44 (4–5), 773–784. https://doi.org/10.1007/S10295-016-1863-2.

Zheng, W., Jiang, L., Lei, Q., Yang, J., Gao, X., Wang, W., Zhang, Y., Kong, T., Chen, Q., Li, G., 2019. Development and validation of quantitative real-time PCR for the detection of residual CHO host cell DNA and optimization of sample pretreatment method in biopharmaceutical products. Biol. Proced. Online 21 (1), 17. https://doi.org/10.1186/s12575-019-0105-1.